

Proteomic responses to metal-induced oxidative stress in
hydrothermal vent-living mussels, *Bathymodiolus* sp., on the
Southwest Indian Ridge

**Catherine Cole^{a,*}, Ana Varela Coelho^b, Rachael H. James^c, Doug Connelly^c
and David Sheehan^d**

^a*Ocean and Earth Science, University of Southampton, European Way, Waterfront Campus,
Southampton, SO14 3ZH, UK*

^b*Instituto de Tecnologia Química e Biológica, Universidade Nova de Lisboa, Av. da
República, 2780-157 Oeiras, Portugal*

^c*National Oceanography Centre, University of Southampton, Waterfront Campus, European
Way, Southampton, SO14 3ZH, UK*

^d*School of Biochemistry and Cell Biology and Environmental Research Institute, University
College Cork, Ireland*

*Corresponding author.

Address: Department of Ocean and Earth Science, University of Southampton, Waterfront
Campus, European Way, Southampton, SO14 3ZH, UK

Telephone: +44 23 80596020

E-mail address: catherine.cole@noc.soton.ac.uk

Article details: Cole, C., Coelho, A. V., James, R. H., Connelly, D., and Sheehan, D. (2014).
Proteomic responses to metal-induced oxidative stress in hydrothermal vent-living mussels,
Bathymodiolus sp., on the Southwest Indian Ridge. *Marine Environmental Research*, 96. 29-
37. DOI: 10.1016/j.marenvres.2013.09.003

1 ABSTRACT

2

3 Bathymodiolin mussels are amongst the dominant fauna occupying hydrothermal vent
4 ecosystems throughout the World's oceans. This subfamily inhabits a highly ephemeral and
5 variable environment, where exceptionally high concentrations of reduced sulphur species
6 and heavy metals necessitate adaptation of specialised detoxification mechanisms. Whilst
7 cellular responses to common anthropogenic pollutants are well-studied in shallow-water
8 species they remain limited in deep-sea vent fauna. *Bathymodiolus* sp. were sampled from
9 two newly-discovered vent sites on the Southwest Indian Ridge (Tiamat and Knuckers Gaff)
10 by the remotely operated vehicle (ROV) Kiel 6000 during the *RRS James Cook* cruise, JC
11 067 in November 2011. Here, we use redox proteomics to investigate the effects of tissue
12 metal accumulation on protein expression and thiol oxidation in gill. Following 2D PAGE,
13 we demonstrate a significant difference in intensity in 30 protein spots in this organ between
14 the two vent sites out of 205 matched spots. We also see significant variations in thiol
15 oxidation in 15 spots, out of 143 matched. At Tiamat, 23 protein spots are up-regulated
16 compared to Knuckers Gaff and we identify 5 of these with important roles in metabolism,
17 cell structure, stress response, and redox homeostasis. We suggest that increased metal
18 exposure triggers changes in the proteome, regulating tissue uptake. This is evident both
19 between vent sites and across a chemical gradient within the Knuckers Gaff vent site. Our
20 findings highlight the importance of proteomic plasticity in successful adaptation to the
21 spatially and temporally fluctuating chemical environments that are characteristic of
22 hydrothermal vent habitats.

23 *Keywords:* Hydrothermal activity; Southwest Indian Ridge; *Bathymodiolus* sp.; Metals;
24 Bioaccumulation; Oxidative stress; Detoxification; Proteome

25 1. Introduction

26 The circulation of conductively-heated seawater in tectonically active regions of the
27 Earth's crust generates high-temperature hydrothermal fluids, which are highly enriched in
28 volatile gases, sulphide and metals, and are discharged through focused and diffuse springs at
29 the seabed (Von Damm *et al.*, 1988). In the mixing zone between hydrothermal fluids and
30 seawater, chemoautotrophic bacteria synthesise organic carbon using reduced compounds
31 (sulphide and methane), supporting a highly productive ecosystem (Stewart *et al.*, 2005;
32 Fisher and Girguis, 2007). Bathymodiolin mussels are amongst the dominant vent fauna
33 inhabiting the hydrothermal environment at the global scale (Miyazaki *et al.*, 2010). These
34 mussels host bacterial endosymbionts in their gills (Cavanaugh *et al.*, 1987; McKiness and
35 Cavanaugh, 2005; Stewart *et al.*, 2005), but they can also feed heterotrophically on
36 particulate organic matter (Page *et al.*, 1991). This mixotrophic diet is an important
37 adaptation to the spatially and temporally fluctuating supply of reducing agents. Adapting to
38 survive in the chemically variable hydrothermal environment also requires an ability to cope
39 with highly toxic concentrations of many metals. In these hydrothermal sites animals are
40 exposed to metal concentrations of the order of a thousand times higher than in oceanic
41 waters (Sarradin *et al.*, 1999) and may have evolved specialised mechanisms of
42 detoxification.

43 Elevated metal exposure can result in oxidative stress in an organism, as some metals
44 lead to production of reactive oxygen species (ROS) which can exceed cellular antioxidant
45 defences (McDonagh *et al.*, 2005). In hydrothermal environments, metals catalyse the
46 oxidation of sulphide to form a number of oxygen- and sulphur-based radicals. This initiates
47 a chain reaction ultimately producing HO•, the most oxidising radical in biological systems
48 (Fridovich, 1998; Tapley *et al.*, 1999). The bulk of ROS are absorbed by proteins and
49 prolonged exposure to metals can therefore cause damaging changes to proteins involved in

50 detoxification. Thiol oxidation is a well-known deleterious proteomic change resulting from
51 the action of ROS produced in response to xenobiotics (Chora *et al.*, 2008; Sheehan *et al.*,
52 2010; Tedesco *et al.*, 2010; 2012; Company *et al.*, 2012). Proteins containing thiol groups (-
53 SH) are critical components of the antioxidant defence system, and are important in enzyme
54 catalysis and in control of the cellular redox environment (Eaton, 2006; Hansen *et al.*, 2009).
55 These groups are particularly susceptible to oxidation, leading to reversible or irreversible
56 formation of a variety of sulphoxidation products. Many of the reversible reactions are
57 integral to protein structure and cell signalling, and they may also provide temporary
58 protection to key functional groups under conditions of oxidative stress (Schafer and
59 Buettner, 2001). The irreversible formation of sulphinic (R-SO₂H) and sulphonic (R-SO₃H)
60 acids are indicative of more severe oxidation (Hansen *et al.*, 2009), and these changes can be
61 detrimental to protein structure and function.

62 Fluorescent labelling of targeted functional groups of amino acid side chains provides
63 a quantitative means of assessing oxidative damage to proteins. Iodoacetamidofluorescein
64 (IAF) reacts with free -SH groups (but not with the oxidised variants) to form stable
65 thioethers. These fluorescein-protein conjugates can be visualised as fluorescent bands/spots
66 in electrophoretic separations (Ahn *et al.*, 1987; Baty *et al.*, 2002). This technique has proved
67 to be a powerful indicator of oxidative stress in *Mytilus edulis* exposed to pro-oxidants
68 (McDonagh and Sheehan, 2007; 2008), but studies in vent organisms are few (Fisher and
69 Girguis, 2007; Mary *et al.*, 2010; Company *et al.*, 2011; 2012).

70 Bathymodiolin mussels inhabit hydrothermal vents in every ocean, and are therefore
71 an ideal genus for enhancing our understanding of proteomic responses to the highly variable
72 environmental stressors characteristic of vent habitats. This study uses redox proteomics to
73 investigate the effect of tissue metal accumulation on protein expression and oxidation in a
74 species of hydrothermal vent-living mussels, *Bathymodiolus* sp., sampled from newly-

75 discovered sites on the Southwest Indian Ridge (SWIR). Hydrothermal ecosystems hosted
76 on the SWIR are of great importance to our understanding of vent-faunal biogeography,
77 owing to the along-axis connections with the Atlantic and Pacific Oceans (German *et al.*,
78 1998; Gamo *et al.*, 2001; Gallant and Von Damm, 2006). Protein-based mechanisms of
79 detoxification are relatively poorly understood in vent fauna, and may form an important
80 piece in the puzzle of vent colonisation, and contribute to understanding the emergence of
81 distinct faunal assemblages throughout the global mid-ocean ridge.

82 2. Materials and methods

83 2.1 *Vent mussel sample collection and preparation*

84 Hydrothermal vent mussels, *Bathymodiolus* sp. (6 – 9 cm), were sampled from two
85 newly-discovered vent sites on the SWIR; Tiamat (37° 47.029' S, 49° 38.965' E, 2770m
86 depth) and Knuckers Gaff (37° 47.030 S, 49° 38.967' E, 2785m depth) by ROV Kiel 6000
87 (GEOMAR) during the *RRS James Cook* cruise JC 067, in November 2011. Whole animals
88 were flash-frozen in liquid nitrogen and stored at -80 °C. Onshore, animals were defrosted
89 on ice and dissected for gill and digestive gland at University College Cork, where all
90 proteomic work was conducted. Bacteria were not removed from dissected tissues. Due to
91 the relatively limited number of animals available (n = 10), samples were not pooled but were
92 homogenised individually in 10 mM Tris-HCl (pH 7.2), 0.5 M sucrose, 0.15 M KCl, 1 mM
93 ethylenediaminetetraacetic acid (EDTA), and 1 mM phenylmethylsulfonyl fluoride (PMSF)
94 using a motor-driven Teflon Potter-Elvehjem homogeniser, and centrifuged at 15,000 x g (60
95 min, 4 °C) to separate the soluble fraction from the pellet. Protein concentration in the
96 supernatant phase was quantified in gill samples using the Bradford method (1976), using
97 bovine serum albumin (BSA) as a calibration standard.

98 2.2 *Analysis of metals in mussel tissues*

99 A number of both essential (Fe, Mn, Cu, Zn) and toxic (Cd, Pb, Hg, As, Al) metals,
100 known to be enriched in hydrothermal fluids relative to seawater, were analysed in gill and
101 digestive gland tissues of *Bathymodiolus* sp. from the soluble and insoluble fractions
102 generated through centrifugation as described in section 2.1. Solid pellets were freeze-dried,
103 and corresponding supernatant fluids were heated to dryness at 130 °C. The dry-weight of
104 the sample was then determined and an aliquot of ~100mg was dissolved in concentrated

105 thermally distilled (TD) HNO₃ by heating in a closed Savillex vial (15ml) on a hotplate at 60
106 °C for ~24 hours. The digested samples were then dried-down at 130 °C and re-dissolved in
107 3% TD HNO₃ spiked with Be (20 ppb), In (5 ppb) and Re (5 ppb) as internal standards.
108 Metal concentrations were determined by inductively coupled plasma mass spectrometry
109 (ICP-MS) (Thermo Scientific X-Series) at the National Oceanography Centre, Southampton.
110 External standards were prepared using 1000 µg ml⁻¹ standard stock solutions (Inorganic
111 Ventures) in 3% TD HNO₃. The precision of the analytical procedure was confirmed through
112 digestion and analysis of certified reference material (CRM); lobster hepatopancreas TORT-1
113 (National Research Council of Canada), alongside the samples. The reproducibility of these
114 analyses was better than 8% for all metals, and measured values for the CRM were within
115 error of the certified values for all metals. The concentrations of metals in the Tris-HCl
116 buffer and HNO₃ were also determined and subtracted from the measured concentrations.
117 Metal concentrations are reported as the sum of the soluble and insoluble fractions, in µg g⁻¹
118 of the tissue dry tissue weight.

119 2.3 *Fluorescein labelling*

120 Protein thiols were labelled with 0.2 mM iodoacetamidofluorescein (IAF) from a 20
121 mM stock solution in dimethyl sulphoxide. Gill sample aliquots containing 25 µg protein
122 (1D PAGE) and 150 µg protein (2D PAGE) were incubated with IAF for two hours on ice in
123 the dark. Proteins were precipitated by incubating extracts in 10% (v/v) trichloroacetic acid
124 (TCA) for 5 min on ice, followed by centrifugation at 11,000 x g for 3 min. The resulting
125 pellet was washed in an excess of ice-cold acetone to remove TCA and any interfering salts
126 or non-protein contaminants. Protein extracts were re-suspended in 15 µl sample buffer for
127 1D PAGE (62.5 mM Tris-HCl (pH 6.8) containing 25% (v/v) glycerol, 2% (w/v) SDS, 5%
128 (v/v) β-mercaptoethanol and a trace amount of bromophenol blue) or 125 µl rehydration

129 buffer for 2D PAGE (7 M urea, 2 M thiourea, 2% (w/v) CHAPS, 4% (v/v) ampholyte
130 (Pharmalyte 3-10), 1.2% (v/v) DeStreak reagent and a trace amount of bromophenol blue).

131 2.4 Polyacrylamide Gel Electrophoresis (PAGE)

132 2.4.1 1D PAGE

133 Gill samples (25 µg protein in 15 µl sample buffer) were heat-denatured and loaded
134 alongside protein molecular mass markers (ThermoScientific, Dublin, Ireland) into wells
135 embedded within a stacking gel of 4.5% (v/v) polyacrylamide in 0.5 M Tris-HCl, pH 6.8, set
136 above a resolving gel of 14% (v/v) polyacrylamide in 1.5 M Tris-HCl, pH 8.8. Gel
137 electrophoresis was carried out at 4 °C using an Atto AE-6450 mini PAGE system (BioRad;
138 Hercules, CA, USA) at a constant voltage of 90 V until samples entered the resolving gel,
139 then 120 V until the dye front reached the bottom of the gel. Fluorescently labelled bands
140 were visualised using a Typhoon Trio+ Variable-Mode Imager (GE Healthcare, Little
141 Chalfont, Bucks, UK) measuring excitation of Fluorescein at 532 nm and emission at 526
142 nm. Protein bands were visualised by colloidal coomassie-staining using the protocol of
143 Dyballa and Metzger (2009).

144 2.4.2 2D PAGE

145 Gill samples (150 µg protein in 125 µl rehydration buffer) were loaded onto 7 cm
146 non-linear immobilised pH gradient (IPG) strips (pH 3 – 10) and rehydrated for 18 hours in
147 the dark at room temperature (Leung *et al.*, 2011). Rehydrated IPG strips were focused on a
148 Protean isoelectric focusing (IEF) cell (Bio-Rad) with linear voltage increases in the
149 following sequence: 250 V for 15 min; 4,000 V for 2 hours; then up to 20,000 Vh. Prior to
150 2D PAGE, focused strips were incubated in equilibration buffer (6M urea, 0.375M tris-HCl,
151 pH 8.8, 2% (w/v) SDS, 20% (v/v) glycerol), first with 2% (w/v) dithiothreitol (DTT) to

152 ensure complete reduction of disulphide bridges and secondly with 2.5% (w/v) iodoacetamide
153 (IAM) to reduce streaking. Equilibrated strips were loaded onto 14% SDS-polyacrylamide
154 gels alongside a wick containing an unstained protein molecular mass marker, and sealed
155 with agarose (0.5%) containing a trace amount of bromophenol blue. Gel electrophoresis
156 was carried out as for 1D PAGE.

157 2.5 *Image Analysis*

158 Coomassie-stained gels were scanned with a calibrated imaging densitometer (GS-
159 800; Bio-Rad). Background subtraction and optical density quantification of protein bands in
160 1D PAGE gels was performed using Quantity One image analysis software (Bio-Rad). For
161 each gel lane, intensity of fluorescence (counts) was normalised against protein content
162 (optical density) to correct for differences in sample loading and enable the extent of thiol
163 oxidation to be compared between samples. Progenesis SameSpots image analysis software
164 (Version 4.5; Nonlinear Dynamics, Durham, NC, USA) was used to align gels, match spots,
165 and quantify spot volumes in 2D PAGE gel images of coomassie-stained, and thiol-labelled
166 protein separations. Spots with a significant change in expression intensity (determined by a
167 fold change of > 1.5 ; $p < 0.05$; student's t-test) between mussels from Tiamat and Knuckers
168 Gaff were selected for protein identification.

169 2.6 *Protein digestion and identification*

170 Proteins were manually picked from 2D PAGE separations, lightly stained with
171 colloidal coomassie. Following in-gel tryptic digestion, extracted peptides were loaded onto
172 a R2 micro-column (RP-C18 equivalent) where they were desalted, concentrated and eluted
173 directly onto a MALDI plate using α -cyano-4-hydroxycinnamic acid (CHCA) as the matrix
174 solution in 50 % (v/v) acetonitrile and 5% (v/v) formic acid. Mass spectra of the peptides

175 were acquired in positive reflectron MS and MS/MS modes using a MALDI-TOF/TOF MS
176 instrument (4800*plus* MALDI TOF/TOF analyzer) with exclusion list of the trypsin autolysis
177 peaks (842.51, 1045.56, 2211.11 and 2225.12). The collected MS and MS/MS spectra were
178 analysed in combined mode by Mascot search engine (version 2.2; Matrix Science, Boston,
179 MA) and the NCBI database restricted to 50 ppm peptide mass tolerance for the parent ions,
180 an error of 0.3 Da for the fragments, one missed cleavage in peptide masses, and
181 carbamidomethylation of Cys and oxidation of Met as fixed and variable amino acid
182 modifications, respectively. No taxonomy restrictions were applied as the genome has not
183 been fully sequenced for species within the *Bathymodiolus* genus. The identified proteins
184 were only considered if a MASCOT score above 95% confidence was obtained ($p < 0.05$)
185 and at least one peptide was identified with a score above 95% confidence ($p < 0.05$). This
186 analysis was conducted by the Analytical Services Unit, Instituto de Tecnologia Química e
187 Biológica (ITQB), New University of Lisbon, Lisbon, Portugal.

188 2.7 *GST* assay

189 Glutathione transferase (GST) activity was quantified in gill tissues ($n = 8$) from
190 sample aliquots containing 15 μg of protein diluted to a volume of 50 μl . Samples were
191 loaded into a 96-well microtitre plate with 100 μl of 2 mM 1-chloro-2,4-dinitrobenzene
192 (CDNB) (from a 40 mM stock in ethanol) in 0.15 M potassium phosphate buffer (pH 6.5).
193 GST activity was measured spectrophotometrically by adding 50 μl of 20 mM reduced
194 glutathione (GSH) and measuring absorbance at 340 nm immediately and every 15 seconds
195 for 5 minutes.

196 GST activity was calculated from the following equation (Habig *et al.*, 1974):

$$197 \quad \text{GST activity } (\mu\text{mol}/\text{min}/\text{mg}) = (\Delta A_{340} V) / (\epsilon l M) \quad (1)$$

198 Where, ΔA_{340} represents the blank-subtracted initial rate of reaction between CDNB
199 and GSH (min^{-1}); V is the volume of reaction (0.2 ml); ϵ is the extinction coefficient of the
200 reaction product at 340 nm ($9.6 \times 10^{-3} \mu\text{M}^{-1} \text{cm}^{-1}$); l is the path length (0.524 cm); and M is
201 the mass of protein (15 μg).

202 2.8 *Statistical Analyses*

203 The distribution of the tissue metal concentrations was significantly different from a
204 normal distribution, so a non-parametric statistical test was required to analyse the variation
205 between groups. Kruskal-Wallis multiple comparison tests (K-W) were applied together with
206 Dunn's post-hoc analysis to quantify the significance of the variation in metal content
207 between gill and digestive gland tissues, both within each vent site and between the two sites.
208 Correlation analyses were conducted to evaluate any relationship between metal
209 concentration and IAF fluorescence counts at each of the two sites. Significant differences in
210 the means of global fluorescence intensity (1D), GST activity, and of coomassie-stained and
211 IAF-labelled spot volumes (2D), in mussel gills between the two vent sites were analysed
212 using the student's t-test after testing for normality in the data. In all cases, significant
213 relationships are reported at the 95% confidence level where $p < 0.05$.

214 3. Results

215 3.1 Tissue metal concentrations

216 Tissue concentrations for essential (Mn, Fe, Cu, Zn) and toxic metals (Al, As, Cd, Hg,
217 Pb) in gill and digestive gland of the hydrothermal vent-living mussel, *Bathymodiolus* sp., for
218 both vent sites are shown in Figure 1. Where significant differences between tissues were
219 observed, gill was found to have higher concentrations of each metal than digestive gland,
220 with the exception of Fe. At the Tiamat vent site, Mn, Zn, Cd, Hg and Pb were all
221 significantly enriched in gill compared with digestive gland at the 95% confidence interval
222 (K-W, $p < 0.05$), whilst Cu was also enriched in gill and Fe enriched in digestive gland at the
223 90% confidence interval (K-W, $p < 0.1$). At the Knuckers Gaff vent site, gill tissues were
224 significantly enriched in Cu, Zn, Cd, Hg and Pb compared with digestive gland (K-W, $p <$
225 0.05). Between the two vent sites, metal concentrations in tissues were consistently higher in
226 mussels sampled from the Knuckers Gaff site compared with those from Tiamat. Whilst
227 large biological variation and small group size, inherent in deep-sea vent sampling, hinders
228 statistical confirmation of these differences, Fe concentrations were found to be significantly
229 higher in gill tissues of mussels from Knuckers Gaff compared with Tiamat (K-W, $p < 0.05$).
230 Aluminium and arsenic showed no statistical variation between tissues or between sites (K-
231 W, $p > 0.05$).

232 3.2 Global thiol oxidation

233 Fluorescence intensity (IAF) measured over 1D PAGE separations, normalised to
234 protein content to correct for any minor differences in sample loading, provides an indication
235 of the global extent of thiol oxidation (Baty *et al.*, 2002) in gill tissues of *Bathymodiolus* sp.
236 (Figure 2). We observed greater fluorescence intensity in IAF-labelled gill samples at
237 Knuckers Gaff ($163,000 \pm 60\%$) compared with Tiamat ($86,400 \pm 9\%$), however this

238 difference was not statistically significant (t-test, $p = 0.16$). Global comparison of the redox
239 modifications to the proteome between the two sites studied is impaired by the extent of
240 biological variation in mussels from Knuckers Gaff. Video footage of the sample collection
241 indicates that individual specimens were collected over a wider area at the Knuckers Gaff
242 vent site compared with Tiamat. Hydrothermal vent habitats are characterised by steep
243 chemical gradients as high-temperature fluids mix with cold seawater, and mussels will be
244 exposed to a spatially variable chemical composition. Greater biological variation in thiol
245 oxidation at Knuckers Gaff may therefore reflect greater chemical diversity within this group
246 compared with Tiamat where individuals were sampled from a more tightly constrained area.
247 In figure S1 (supplementary material) the relationship between global thiol oxidation and
248 tissue metal content in gills of individual animals is analysed for each site. Correlation
249 analyses between metal concentration and coomassie-normalised fluorescence counts (1D
250 PAGE) reveal a number of significant relationships. IAF counts decrease significantly with
251 increasing As at Tiamat ($R = -0.895$; $p < 0.05$) and Fe at Knuckers Gaff ($R = -0.895$; $p <$
252 0.05), but increase significantly with increasing Pb at Tiamat ($R = 0.957$; $p < 0.05$).

253 3.3 Protein expression profiles: 2D PAGE

254 Whilst the 1D PAGE approach discussed in Section 3.2 provides a global indication
255 of thiol oxidation status in tissues, it does not readily distinguish effects at the level of
256 individual proteins. The response of individual proteins to oxidative stress can be better
257 assessed using 2D PAGE. As metal concentration in this study was found to be higher in gill
258 than digestive gland, we focused on 2D PAGE analysis of IAF-labelled proteins in gill tissues
259 (Figure 3).

260 Excluding smears and gel defects, a total of 205 well-resolved spots were matched in
261 coomassie-stained protein separations between the two groups. A significant difference in

262 signal level between the two sites was measured in 30 protein spots ($p < 0.05$), of which 10
263 were highly significant ($p < 0.01$). Of these, 23 spots were elevated at Tiamat and 7 were
264 elevated at Knuckers Gaff (Figure 4). Successful protein identifications are presented in
265 Table 1. In fluorescent scans of the same gels, a total of 143 IAF-labelled spots were
266 matched in gill, and 15 of these showed a significant difference in spot volume between the
267 two vent sites ($p < 0.05$). At Tiamat, 10 spots showed a reduction in fluorescence with IAF
268 in comparison with Knuckers Gaff, whilst 5 spots showed an increase (Figure 4). These
269 changes in fluorescence intensity occurred independently of any significant change in protein
270 expression, suggesting redox modification to proteins present in all 15 spots.

271 3.4 *GST activity*

272 GST activity was found to be higher in gills from *Bathymodiolus* sp. at Tiamat (0.085
273 ± 0.03) compared to Knuckers Gaff (0.043 ± 0.03), though statistical comparison of the
274 means of each group revealed that this difference was only significant at the 90% confidence
275 level (t-test; $p = 0.094$).

276

277 4. Discussion

278 Bathymodiolin mussels are amongst the dominant fauna occupying hydrothermal vent
279 ecosystems throughout the world's oceans (Fisher *et al.*, 1988; Desbruyères *et al.*, 2000;
280 Cuvelier *et al.*, 2009; Miyazaki *et al.*, 2010). In these deep-sea vent environments,
281 environmental stressors are manifold and extreme exposure to heavy metals may have
282 necessitated the adaptation of specialised mechanisms of detoxification. In particular, metals
283 trigger the production of ROS, which can disturb the cellular redox balance and lead to
284 oxidative stress (Sheehan, 2006; Hansen *et al.*, 2009). A ubiquitous cellular strategy for
285 detoxification involves the binding of metals to specific low molecular mass, thiol-containing
286 proteins known as metallothioneins (MT) (Viarengo and Nott, 1993), and MT expression has
287 been well-studied in *Bathymodiolus* spp. (Geret *et al.*, 1998; Company *et al.*, 2006; 2010;
288 Hardivillier *et al.*, 2006; Martins *et al.*, 2011). Oxidative stress also stimulates redox
289 modifications to proteins involved in detoxification, and can detrimentally influence protein
290 structure and function (Berlett and Stadtman, 1997). Whilst redox proteomics has frequently
291 been employed in ecotoxicological studies with shallow-water animals (e.g. Manduzio *et al.*,
292 2005; McDonagh *et al.*, 2006; McDonagh and Sheehan, 2007; 2008; Chora *et al.*, 2008;
293 Tedesco *et al.*, 2010), studies in vent fauna are comparatively rare (Company *et al.*, 2011;
294 2012).

295 Mussels from Knuckers Gaff appear to have a higher metal load in their tissues, but a
296 larger sample group would be needed to test whether this is significant, representing a
297 considerable challenge for deep-sea, remote sampling. Statistical tests performed here
298 indicate that tissue metal concentrations are generally similar between the two groups, with
299 the exception of iron in gill. Higher concentrations of Fe in gill at Knuckers Gaff could
300 indicate greater bioavailability of this element, potentially through a higher hydrothermal
301 flux, or may reflect a slower rate of removal. Two-dimensional PAGE separations of gill

302 proteins revealed significant changes in intensity of 30 spots between the two vent sites, of
303 which 23 were more intense at Tiamat and 7 were more intense at Knuckers Gaff. Whilst it
304 is difficult to elucidate whether these changes indicate suppression of protein expression in
305 response to greater xenobiotic stress at one site, or up-regulation of proteins involved in
306 antioxidant defence at the other, it is clear that the proteome of *Bathymodiolus* sp. is highly
307 sensitive to changes in chemical environment, as previously observed with *B. azoricus* on the
308 Mid-Atlantic Ridge (Company *et al.*, 2011). Significant differences in the thiol subproteome
309 were also observed between the two groups, with 10 spots showing reduced intensity at
310 Tiamat, and 5 showing greater intensity. Reduced IAF-associated fluorescence may reflect
311 greater thiol oxidation, but may also indicate lower abundance of thiol-containing proteins.
312 In this study, changes in spot intensity with IAF occurred independently of differences in
313 intensity with coomassie, therefore it may be that the thiol subproteome of Tiamat mussels is
314 more sensitive to oxidant attack than at Knuckers Gaff.

315 Exposure to metal-induced ROS has previously been shown to trigger up-regulation
316 of numerous antioxidant enzymes in hydrothermal vent fauna (Company *et al.*, 2004; 2006;
317 2010; Marie *et al.*, 2006; Gonzalez-Rey *et al.*, 2007). However, few studies have applied a
318 redox proteomic approach to screen for changes in expression and oxidative transformations
319 of individual proteins involved in key biological structures and processes (Boutet *et al.*, 2009;
320 Mary *et al.*, 2010; Company *et al.*, 2011; 2012). Identifying individual proteins in deep-sea
321 vent fauna is challenging owing to the relative paucity in their genome information.
322 Nevertheless, we report enhanced expression of S-adenosylhomocysteine hydrolase (SAHH),
323 alpha enolase, glutamine synthetase type I, actin, and fumarylacetoacetate hydrolase (FAH)
324 in gill tissues of *Bathymodiolus* sp. sampled at Tiamat compared to those sampled at
325 Knuckers Gaff. These proteins occupy diverse roles in metabolism, cell structure, stress

326 response and redox homeostasis and may be variably regulated in response to conditions of
327 oxidative stress.

328 SAHH is a cytosolic enzyme with an important antioxidant role owing to its
329 involvement in regulating the synthesis of GSH via metabolism and regeneration of cysteine
330 and methionine (Kloor *et al.*, 2000; Martinov *et al.*, 2010; Liao *et al.*, 2012), and in regulating
331 biological transmethylation (Turner *et al.*, 2000). Enhanced expression of this enzyme has
332 previously been linked to oxidative stress caused by metal exposure (Bagnyukova *et al.*,
333 2007), and has been identified as a stress response in hydrothermal vent mussels, *B. azoricus*
334 from the Mid-Atlantic Ridge (Company *et al.*, 2011), and *B. thermophilus* from the East
335 Pacific Rise (Boutet *et al.*, 2009). Alpha enolase, a cytosolic enzyme, is both abundant and
336 highly conserved in eukaryotic and prokaryotic organisms owing to its critical role in
337 carbohydrate catabolism via the glycolytic pathway (Pancholi, 2001). Alpha enolase has also
338 been found to protect cells from oxidative and thermal stress, functioning as a hypoxic stress
339 protein (Aaronson *et al.*, 1995) and a heat shock protein (Iida and Yahara, 1985), and can be
340 considered as a marker of pathological stress with multiple stress response roles (Díaz-Ramos
341 *et al.*, 2012). Glutamine synthetase type I is exclusive to prokaryotes and must therefore
342 derive from the bacterial symbionts hosted in gill tissue. Elevated expression of this bacterial
343 protein may indicate a greater population of gill endosymbionts at Tiamat in response to a
344 greater exposure to reduced substrates. Actin is an abundant cytoskeletal protein in
345 eukaryotic cells, polymerising to form a network of microfilaments with numerous functions
346 including cell motility, cell division, cell signalling and protein synthesis (Pollard and
347 Cooper, 1986). Actin is highly sensitive to oxidant attack (Dalle-Donne *et al.*, 2001) and has
348 been shown in many studies to be a target of oxidative stress in bivalves inhabiting both
349 shallow-water (Rodríguez-Ortega *et al.*, 2003; Manduzio *et al.*, 2005; McDonagh *et al.*, 2005;
350 McDonagh and Sheehan, 2007; 2008; Chora *et al.*, 2009) and hydrothermal vent

351 environments (Company *et al.*, 2011). Under moderate conditions of oxidative stress, the
352 formation of disulphide bonds between cysteine sulphydryl groups in actin and those of GSH,
353 prevents excessive intra-molecular polymerisation and enables microfilament preservation
354 (Dalle-Donne *et al.*, 2001). Thus, actin not only responds to ROS-induced stress but may be
355 actively involved in buffering potential damage to cells. FAH is one of just ten enzymes
356 known to have the capacity to hydrolyse carbon-carbon bonds in aromatic amino acids
357 (Timm *et al.*, 1999). It is involved in the catabolism of tyrosine and phenylalanine,
358 catalysing the cleavage of fumerylacetoacetate in the final step of this essential metabolic
359 pathway (Bateman *et al.*, 2001). This enzyme is more abundant in mussels sampled from
360 Tiamat compared with Knuckers Gaff, perhaps reflecting greater need for efficient break
361 down of tyrosine metabolites which can further contribute to oxidative stress in cells (Fisher
362 *et al.*, 2008).

363 GST activity is also enhanced in gills of mussels from Tiamat compared with
364 Knuckers Gaff, though this difference is only significant at the 90% confidence interval ($p <$
365 0.1). GST is a key enzyme involved in phase II detoxification, which catalyses conjugation
366 of GSH to electrophilic centres on a range of xenobiotic substrates, facilitating their
367 dissolution and subsequent excretion from the organism (Strange *et al.*, 2001). Elevated
368 expression of GST, and of proteins involved in diverse cellular processes (discussed above),
369 suggests that mussels at Tiamat may have a greater battery of defences against xenobiotic
370 substrates.

371 A recent study has shown that hydrothermal vent mussels from the Mid-Atlantic
372 Ridge, *B. azoricus*, differ in their systems of antioxidant defence depending on the specific
373 environmental conditions to which they are exposed (Company *et al.*, 2012). *Bathymodiolus*
374 sp. sampled from the SWIR in this study demonstrate significant proteomic variability
375 between two vent sites. We measure enhanced expression of a number of proteins involved

376 in redox homeostasis at Tiamat, suggesting that chemical stress may in fact be greater at this
377 site than at Knuckers Gaff. We also observe an increase in oxidative modifications to the
378 thiol subproteome in mussels from Tiamat compared with Knuckers Gaff, further indicating a
379 higher metal environment. Elevated exposure to metals is known to trigger the up-regulation
380 of metal-binding proteins, facilitating excretion (Langston *et al.*, 1998). It is possible that
381 mussels from Tiamat experience greater exposure to metals, but maintain redox homeostasis
382 through enhanced induction of GST and other antioxidant enzymes. Consequently, metal
383 concentrations in tissues are regulated at a similar level to those in mussels at the Knuckers
384 Gaff site.

385 Gill tissues of mussels from both Tiamat and Knuckers Gaff were found to contain
386 higher concentrations of many of the metals analysed compared with digestive gland. This
387 suggests greater exposure of gill to bioavailable metals in seawater and supports a primary
388 feeding mechanism of chemoautotrophy via endosymbiotic bacteria (Fiala-Médioni *et al.*,
389 2002; Duperron *et al.*, 2006; Riou *et al.*, 2008). Mussels in this study were sampled from
390 active chimney structures where methane and sulphide are likely to have been in plentiful
391 supply. Whilst Bathymodiolin mussels have a mixotrophic diet in which their energy
392 requirements can be maintained both by symbionts in their gills and by suspension feeding on
393 particulate organic matter (Le Pennec *et al.*, 1990), filter feeding may be negligible as
394 mussels increase in size and proximity to the vent (Martins *et al.*, 2008; De Brusserolles *et*
395 *al.*, 2009). Gill tissue represents the direct interface between environmental metals and
396 cellular physiology, and studies with *B. azoricus* collected from Mid-Atlantic Ridge vent sites
397 have also shown a greater metal burden in gill compared with digestive gland (Geret *et al.*,
398 1998; Kadar *et al.*, 2005; Cosson *et al.*, 2008). Whilst accumulation in digestive gland is
399 considerably greater in vent mussels compared with non-vent fauna, reflecting long-term
400 metal exposure (Cosson *et al.*, 2008; Chora *et al.*, 2009; Martins *et al.*, 2011), higher MT

401 concentrations in this organ compared with gill enable greater metal regulation (Langston *et*
402 *al.*, 1998).

403

404 **5. Conclusions**

405 This is the first study to incorporate a redox proteomics approach to investigate stress
406 tolerance in hydrothermal vent mussels (*Bathymodiolus* sp.) collected from the Southwest
407 Indian Ridge. Although, as yet, no environmental or fluid chemistry data are available for
408 these sites, there is significant variability in the proteome between Tiamat and Knuckers
409 Gaff, including the expression of proteins involved in a range of metabolic and detoxification
410 processes, which is likely to reflect variability in response to environmental stressors. Gills
411 were found to be significantly enriched relative to digestive gland in Mn, Zn, Cd, Hg and Pb
412 at Tiamat, and Cu, Zn, Cd, Hg and Pb at Knuckers Gaff, indicating enhanced exposure of this
413 tissue to bioavailable metals, and may indicate a greater reliance on the gill for nutrition via
414 chemoautotrophic endosymbionts at both sites. At Knuckers Gaff, biological variation was
415 very high in all analyses of metal content, protein expression and redox changes to the
416 proteome. Mussels sampled at this site cover a wider geographic area, and consequently they
417 are likely to have experienced more variation in their exposure to toxic compounds. This
418 study highlights the variable proteomic response of *Bathymodiolus* sp. to a rapidly fluctuating
419 and highly ephemeral chemical environment, and demonstrates the sensitivity of the redox
420 proteomic approach to evaluating stress response between vent habitats within the same
421 hydrothermal system. We identify five proteins as potential markers of oxidative stress in
422 *Bathymodiolus* sp., and demonstrate the importance of proteomic plasticity in adaptation to
423 the hydrothermal vent habitat.

424

425 **6. Acknowledgements**

426 We thank the Captain and crew of the *RRS James Cook* and the ROV Kiel 6000
427 technical team for facilitating sample collection during JC 067; Dr Jon Copley and Leigh
428 Marsh for ship-board sample preparation; and the Biochemical Department of University
429 College Cork, particularly Louis Charles-Rainville and Tahira Ja'afar for their laboratory
430 support. This work was funded by the Natural Environment Research Council (NERC)
431 National Capability Programme and the Graduate School of the National Oceanography
432 Centre (GSNOCS), NERC and University of Southampton.

433 **7. Author Contributions**

434 C. C., R. H. J., D. C., and D. S. jointly conceived this study and designed the analytical
435 approach. The proteomic analyses were performed by C. C. and A. V. C., and the metal
436 analyses by C. C. All authors contributed to the writing of the manuscript.

437 **8. References**

438 Aaronson, R., Graven, K., Tucci, M., McDonald, R., Farber, H., 1995. Non-neuronal
439 enolase is an endothelial hypoxic stress protein. *The Journal of Biological Chemistry* 270,
440 27752 – 27757.

441 Ahn, B., Rhee, S.G., Stadtman, E. R., 1987. Use of Fluorescein hydrazide and
442 fluorescein thiosemicarbazide reagents for the fluorometric determination of protein carbonyl
443 groups and for the detection of oxidised protein on polyacrylamide gels. *Analytical*
444 *Biochemistry* 161, 245 – 257.

445 Bagnyukova, T., Luzhna, L., Pogribny, I., Lushchak, V., 2007. Oxidative stress and
446 antioxidant defences in goldfish liver in response to short-term exposure to arsenite.
447 *Environmental and Molecular Mutagenesis* 48, 658 – 665.

448 Bateman, R., Bhanumorthy, P., Witte, J., McClard, R., Grompe, M., Timm, D.,
449 2001. Mechanistic inferences from the crystal structure of fumarlyacetate hydrolase with a
450 bound phosphorus-based inhibitor. *The Journal of Biological Chemistry* 276, 15284 – 15291.

451 Baty, J. W., Hampton, M. B., Winterbourn, C. C., 2002. Detection of oxidant
452 sensitive thiol proteins by fluorescence labelling and two-dimensional electrophoresis.
453 *Proteomics* 2, 1261 – 1266.

454 Berlett, B. S., Stadtman, E. R., 1997. Protein oxidation in aging, disease, and
455 oxidative stress. *The Journal of Biological Chemistry* 272, 20313 – 20316.

456 Boutet, I., Jollivet, D., Shillito, B., Moraga, D., Tanguy, A., 2009. Molecular
457 identification of differently regulated genes in the hydrothermal-vent species *Bathymodiolus*
458 *thermophilus* and *Paralvinella pandorae* in response to temperature. *BMC Genomics* 10,
459 doi: 10.1186/1471-2164-10-222

460 Bradford, M., 1976. A rapid and sensitive method for the quantification of microgram
461 quantities of protein utilizing the principle of protein-dye binding. *Analytical Biochemistry*
462 72, 248 – 254.

463 Cavanaugh, C., Levering, P., Maki, J., Mitchell, R., Lidstrom, M., 1987. Symbiosis
464 of methylophilic bacteria and deep-sea mussels. *Nature* 325, 346 – 348.

465 Chora, S., McDonagh, B., Sheehan, D., Starita-Geribaldi, M., Roméo, M., Bebianno,
466 M. J., 2008. Ubiquitination and carbonylation as markers of oxidative-stress in *Ruditapes*
467 *decussatus*. *Marine Environmental Research* 66, 95 – 97.

468 Chora, S., Starita-Geribaldi, M., Guignonia, J-M., Samson, M., Roméo, M., and
469 Bebianno, M. J., 2009. Effect of cadmium in the clam *Ruditapes decussatus* assessed by
470 proteomic analysis. *Aquatic Toxicology* 94, 300 – 308.

471 Company, R., Serafim, A., Bebianno, M. J., Cosson, R., Shillito, B., Fiala-Médioni,
472 A., 2004. Effect of cadmium, copper and mercury on antioxidant enzyme activities and lipid
473 peroxidation in the gills of the hydrothermal vent mussel *Bathymodiolus azoricus*. *Marine*
474 *Environmental Research* 58, 377 – 381.

475 Company, R., Serafim, A., Cosson, R., Camus, L., Shillito, B., Fiala-Médioni, A.,
476 Bebianno, M. J., 2006. The effect of cadmium on antioxidant responses and the
477 susceptibility to oxidative stress in the hydrothermal vent mussel *Bathymodiolus azoricus*.
478 *Marine Biology* 148, 817 – 825.

479 Company, R., Serafim, A., Cosson, R. P., Fiala-Médioni, A., Camus, L., Serrão-
480 Santos, R., Bebianno, M. J., 2010. Sub-lethal effects of cadmium on the antioxidant defence

481 system of the hydrothermal vent mussel *Bathymodiolus azoricus*. Ecotoxicology and
482 Environmental Safety 73, 788 – 795.

483 Company, R., Antúnez, O., Bebianno, M., Cajaraville, M., Torreblanca, A., 2011. 2-
484 D difference gel electrophoresis approach to assess protein expression profiles in
485 *Bathymodiolus azoricus* from Mid-Atlantic Ridge hydrothermal vents. Journal of Proteomics
486 74, 2909 – 2919.

487 Company, R., Torreblanca, A., Cajaraville, M., Bebianno, M. J., Sheehan, D., 2012.
488 Comparison of thiol subproteome of the vent mussel *Bathymodiolus azoricus* from different
489 Mid-Atlantic Ridge vent sites. Science of the Total Environment, 437, 413 – 421.

490 Cosson, R. P., Thiébaud, É., Company, R., Castrec-Rouelle, M., Colaço, A., Martins,
491 I., Sarradin, P-M., Bebianno M. J., 2008. Spatial variation of metal bioaccumulation in the
492 hydrothermal vent mussel *Bathymodiolus azoricus*. Marine Environmental Research 65, 405
493 – 415.

494 Cuvelier, D., Sarrazin, J., Colaço, A., Copley, J., Desbruyères, D., Glover, A. G.,
495 Tyler, P., Serrão-Santos, R., 2009. Distribution and spatial variation of hydrothermal faunal
496 assemblages at Lucky Strike (Mid-Atlantic Ridge) revealed by high-resolution video image
497 analysis. Deep-Sea Research I 56, 2026 – 2040.

498 Dalle-Donne, I., Rossi, R., Milzani, A., Simplicio, P., Colombo, R., 2001. The actin
499 cytoskeleton response to oxidants: from small heat shock protein phosphorylation to changes
500 in the redox state of actin itself. Free Radical Biology and Medicine 31, 1624 – 1632.

501 De Brusserolles, F., Sarrazin, J., Gauthier, O., Gélinas, Y., Fabri, M. C., Sarradin, P.
502 M., Desbruyères, D., 2009. Are spatial variations in the diets of hydrothermal fauna linked to
503 local environmental conditions? Deep-Sea Research II 56, 1649 – 1664.

504 Desbruyères, D., Almerida, A., Biscoito, M., Comtet, T., Khripounoff, A., Le Bris,
505 N., Sarradin, P. M., Segonzac, M., 2000. A review of the distribution of hydrothermal vent
506 communities along the northern Mid-Atlantic Ridge: dispersal vs. environmental controls.
507 Hydrobiologia 440, 201 – 216.

508 Díaz-Ramos, A., Roig-Borrellas, A., García-Melero, A., López-Aleman, R., 2012.
509 α -enolase, a multifunctional protein: It's role on pathophysiological situations. Journal of
510 Biomedicine and Biotechnology 2012, doi: 10.1155/2012/156795.

511 Duperron, S., Bergin, C., Zielinski, F., Blazejak, A., Pernthaler, A., McKiness, Z. P.,
512 DeChaine, E., Cavanaugh, C. M., Dubilier, N., 2006. A dual symbiosis shared by two mussel
513 species, *Bathymodiolus azoricus* and *Bathymodiolus puteoserpentis* (Bivalvia: Mytilidae),
514 from hydrothermal vents along the northern Mid-Atlantic Ridge. *Environmental*
515 *Microbiology* 8, 1441 – 1447.

516 Dyballa, N., Metzger, S., 2009. Fast and sensitive colloidal coomassie G-250 staining
517 for proteins in polyacrylamide gels. *Journal of Visualized Experiments* 30.
518 <http://www.jove.com/details.php?id=1431>, doi: 10.3791/1431.

519 Eaton, P., 2006. Protein thiol oxidation in health and disease: Techniques for
520 measuring disulfides and related modifications in complex protein mixtures. *Free Radical*
521 *Biology and Medicine* 40, 1889 – 1899.

522 Fiala-Médioni, A., McKiness, Z. P., Dando, P., Boulegue, J., Mariotti, A., Alayse-
523 Danet, A. M., Robinson, J. J., Cavanaugh, C. M., 2002. Ultrastructural, biochemical, and
524 immunological characterisation of two populations of the mytilid mussel *Bathymodiolus*
525 *azoricus* from the Mid-Atlantic Ridge: evidence for a dual symbiosis. *Marine Biology* 141,
526 1035 – 1043.

527 Fisher, C. R., Childress, J. J., Arp, A. J., Brooks, J. M., Distel, D., Favuzzi, J. A.,
528 Felbeck, H., Hessler, R., Johnson, K. S., Kennicutt, M. C., Macko, S. A., Newton, A., Powell,
529 M. A., Somero, G. N., Soto, T., 1988. Microhabitat variation in the hydrothermal vent
530 mussel, *Bathymodiolus thermophilus*, at the Rose Garden vent on the Galapagos Rift. *Deep-*
531 *Sea Research* 35, 1769 – 1791.

532 Fisher, C., Girguis, P., 2007. A proteomic snapshot of life at a vent. *Science* 315, 198
533 – 199.

534 Fisher, A., Page, K., Lithgow, G., Nash, L., 2008. The *Caenorhabditis elegans*
535 K10C2.4 gene encodes a member of the fumarylacetoacetate hydrolase family. *The Journal*
536 *of Biological Chemistry* 283, 9127 – 9135.

537 Fridovich, I., 1998. Oxygen Toxicity: A radical explanation. *The Journal of*
538 *Experimental Biology* 201, 1203 – 1209.

539 Gallant, R., Von Damm, K., 2006. Geochemical controls on hydrothermal fluids from
540 the Kairei and Edmond vent fields, 23°-25°S, Central Indian Ridge. *Geochemistry,*
541 *Geophysics, Geosystems* 7, Q06018, doi:10.1029/2005GC001067

542 Gamo, T., Chiba, H., Yamanaka, T., Okudaira, T., Hashimoto, J., Tsuchida, S.,
543 Ishibashi, J., Kataoka, S., Tsunogai, U., Okamura, K., Sano, Y., Shinjo, R., 2001. Chemical
544 characteristics of newly discovered black smoker fluids and associated hydrothermal plumes
545 at the Rodriguez Triple Junction, Central Indian Ridge. *Earth and Planetary Science Letters*
546 193, 371 – 379.

547 Geret, F., Rousse, N., Riso, R., Sarradin, P-M., and Cosson, R. P., 1998. Metal
548 compartmentalisation and metallothionein isoforms in mussels from the Mid-Atlantic Ridge;
549 preliminary approach to the fluid-organism relationship. *Cahiers de Biologie Marine* 39, 291
550 – 293.

551 German, C., Baker, E., Tamaki, K., FUJI Science Team, 1998. Hydrothermal activity
552 along the southwest Indian Ridge. *Nature* 395, 490 – 493.

553 Gonzalez-Rey, M., Serafim, A., Company, R., Gomes, T., Bebianno, M. J., 2008.
554 Detoxification mechanisms in shrimp: Comparative approach between hydrothermal vent
555 fields and estuarine environments. *Marine Environmental Research* 66, 35 – 37.

556 Habig, W. H., Pabst, M. J., Jakoby, W. B., 1974. Glutathione S-Transferases: The
557 first step in mercapturic acid formation. *Journal of Biological Chemistry* 249, 7130 – 7139.

558 Hansen, R. E., Roth, D., Winther, J. R., 2009. Quantifying the global cellular thiol-
559 disulphide status. *Proceedings of the National Academy of Science* 106, 422 – 427.

560 Hardivillier, Y., Denis, F., Demattei, M-V., Bustamante, P., Laulier, M., Cosson, R.,
561 2006. Metal influence on metallothionein synthesis in the hydrothermal vent mussel
562 *Bathymodiolus thermophilus*. *Comparative Biochemistry and Physiology, Part C* 143, 321 –
563 332.

564 Iida, H., Yahara, I., 1985. Yeast heat-shock protein of M, 48,000 is an isoprotein of
565 enolase. *Nature* 315, 688 – 690.

566 Kádár, E., Costa, V., Santos, R. S., Lopes, H., 2005. Behavioural response to the
567 bioavailability of inorganic mercury in the hydrothermal mussel *Bathymodiolus azoricus*.
568 *The Journal of Experimental Biology* 208, 505 – 513.

569 Kloor, D., Yao, K., Delabar, U., Osswald, H., 2000. Simple and sensitive binding
570 assay for measurement of adenosine using reduced S-adenosylhomocysteine hydrolase.
571 *Clinical Chemistry* 46, 537 – 542.

572 Langston, W. J., Bebianno, M. J., Burt, G. R., 1998. Metal handling strategies in
573 molluscs, in: Langston, W. J., Bebianno, M. J. (Eds.), Metal Metabolism in Aquatic
574 Environments. Chapman & Hall, London, pp. 219-283.

575 Le Pennec, M., Donval, A., Herry, A., 1990. Nutritional strategies of the
576 hydrothermal ecosystem bivalves. Progress in Oceanography 24, 71 – 80.

577 Leung, P., Wang, Y., Mak, S., Ng, W. C., Leung, K., 2011. Differential proteomic
578 responses in hepatopancreas and adductor muscles of the green-lipped mussel *Perna viridis*
579 to stresses induced by cadmium and hydrogen peroxide. Aquatic Toxicology 105, 49 – 61.

580 Liao, S., Li, R., Shi, L., Wang, J., Shang, J., Zhu, P., Chen, B., 2012. Functional
581 analysis of an S-adenosylhomocysteine hydrolase homolog of chestnut blight fungus. FEMS
582 Microbiology Letters 336, 64 – 72.

583 Manduzio, H., Cosette, P., Gricourt, L., Jouenne, T., Lenz, C., Andersen, O-K.,
584 Leboulenger, F., Rocher, B., 2005. Proteome modifications of blue mussel (*Mytilus edulis*
585 L.) gills as an effect of water pollution. Proteomics 5, 4958 – 4963.

586 Marie, B., Genard, B., Rees, J-F., Zaul, F., 2006. Effect of ambient oxygen
587 concentration on activities of enzymatic antioxidant defences and aerobic metabolism in the
588 hydrothermal vent worm, *Paralvinella grasslei*. Marine Biology 150, 273 – 284.

589 Martinov, M., Vitvitsky, V., Banerjee, R., Ataullakhanov, F., 2010. The logic of the
590 hepatic methionine metabolic cycle. Biochimica et Biophysica Acta 1804, 89 – 96.

591 Martins, I., Colaço, A., Dando, P. R., Martins, I., Desbruyères, D., Sarradin, P-M.,
592 Marques, J. C., Serrão-Santos, R., 2008. Size-dependent variations on the nutritional
593 pathway of *Bathymodiulus azoricus* demonstrated by a C-flux model. Ecological Modelling
594 217, 59 – 71.

595 Martins, I., Cosson, R. P., Riou, V., Sarradin, P-M., Sarrazin, J., Serrão-Santos, R.,
596 Colaço, A., 2011. Relationship between metal levels in the vent mussel *Bathymodiulus*
597 *azoricus* and local microhabitat chemical characteristics of Eiffel Tower (Lucky Strike).
598 Deep-Sea Research I 58, 306 – 315.

599 Mary, J., Rogniaux, H., Rees, J-F, Zal, F., 2010. Response of *Alvinella pompejana* to
600 variable oxygen stress: A proteomic approach. Proteomics 10, 2250 – 2258.

601 McDonagh, B., Tyther, R., Sheehan, D., 2005. Carbonylation and glutathionylation
602 of proteins in the blue mussel *Mytilus edulis* detected by proteomic analysis and Western
603 blotting: Actin as a target for oxidative stress. *Aquatic Toxicology* 73, 315 – 326.

604 McDonagh, B., Tyther, R., Sheehan, D., 2006. Redox proteomics in the mussel,
605 *Mytilus edulis*. *Marine Environmental Research* 62, S101 – S104.

606 McDonagh, B., Sheehan, D., 2007. Effect of oxidative stress on protein thiols in the
607 blue mussel *Mytilus edulis*: Proteomic identification of target proteins. *Proteomics* 7, 3395 –
608 3403.

609 McDonagh, B., Sheehan, D., 2008. Effects of oxidative stress on protein thiols and
610 disulphides in *Mytilus edulis* revealed by proteomics: Actin and protein disulphide isomerase
611 are redox targets. *Marine Environmental Research* 66, 193 – 195.

612 McKiness, Z., Cavanaugh, C., 2005. The ubiquitous mussel: *Bathymodiolus* aff.
613 *brevior* symbiosis at the Central Indian Ridge hydrothermal vents. *Marine Ecology Progress*
614 *Series* 295, 183 – 190.

615 Miyazaki, J-I., de Oliveria Martins, L., Fujita, Y., Matsumoto, H., Fujiwara, Y., 2010.
616 Evolutionary process of deep-sea *Bathymodiolus* mussels. *PLoS ONE* 5(4): e10363.
617 doi:10.1371/journal.pone.0010363.

618 Page, H., Fiala-Medioni, A., Fisher, C., Childress, J., 1991. Experimental evidence
619 for filter-feeding by the hydrothermal vent mussel, *Bathmodiolus thermophilus*. *Deep-Sea*
620 *Research* 38, 1455 – 1461.

621 Pancholi, V., 2001. Multifunctional α -enolase: its role in diseases. *Cellular and*
622 *Molecular Life Sciences* 58, 902 – 920.

623 Pollard, T., Cooper, J., 1986. Actin and actin-binding proteins. A critical evaluation
624 of mechanisms and functions. *Annual Reviews of Biochemistry* 55, 987 – 1035.

625 Riou, V., Halary, S., Duperron, S., Bouillon, S., Elskens, M., Bettencourt, R., Santos,
626 R. S., Dehairs, F., Colaço, A., 2008. Influence of CH₄ and H₂S availability on symbionts
627 distribution, carbon assimilation and transfer in the dual symbiotic vent mussel
628 *Bathymodiolus azoricus*. *Biogeosciences* 5, 1681 – 1691.

629 Rodríguez-Ortega, M., Grosvik, B., Rodríguez-Ariza, A., Goksoyr, A., López-Barea,
630 J., 2003. Changes in protein expression profiles in bivalve molluscs (*Chamaelea gallina*)
631 exposed to four model environmental pollutants. *Proteomics* 3, 1535 – 1543.

632 Sarradin, P-M., Caprais, J-C., Riso, R., Kerouel, R., Aminot, A., 1999. Chemical
633 environment of the hydrothermal mussel communities in the Lucky Strike and Menez Gwen
634 vent fields, Mid Atlantic Ridge. *Cahiers de Biologie Marine* 40, 93 – 104.

635 Schafer, F. Q., Buettner, G. R., 2001. Redox environment of the cell as viewed
636 through the redox state of the glutathione disulfide/glutathione couple. *Free Radical Biology*
637 *and Medicine* 30, 1191 – 1212.

638 Sheehan, D. 2006. Detection of redox-based modification in two-dimensional
639 electrophoresis proteomic separations. *Biochemical and Biophysical Research*
640 *Communications* 349, 455 – 462.

641 Sheehan, D., McDonagh, B., Barcena, J. A., 2010. Redox Proteomics. *Expert*
642 *Reviews of Proteomics* 7, 1 – 4.

643 Strange, R. C., Spiteri, M. A., Ramachandran, S., Fryer, A. A., 2001. Glutathione-S-
644 transferase family of enzymes. *Mutation Research* 482, 21 – 26.

645 Stewart, F., Newton, I., Cavanaugh, C., 2005. Chemosynthetic endosymbioses:
646 adaptations to oxic-anoxic interfaces. *Trends in Microbiology* 13, 439 – 448.

647 Tapley, D., Buettner, G. R., Shick, J. M., 1999. Free radicals and chemiluminescence
648 as products of the spontaneous oxidation of sulphide in seawater, and their biological
649 implications. *Biology Bulletin* 196, 52 – 56.

650 Tedesco, S., Doyle, H., Blasco, J., Redmond, G., Sheehan, D., 2010. Oxidative stress
651 and toxicity of gold nanoparticles in *Mytilus edulis*. *Aquatic Toxicology* 100, 178 – 186.

652 Tedesco, S., Jaafar, S.N.T., Coelho A.V., Sheehan D. 2012. Protein thiols as novel
653 biomarkers in ecotoxicology: A case study of oxidative stress in *Mytilus edulis* sampled near
654 a former industrial site in Cork Harbour, Ireland. *Journal of Integrated Omics* 2, 39 - 47.

655 Timm, D., Mueller, H., Bhanumoorthy, P., Harp, J., Bunick, G., 1999. Crystal
656 structure and mechanism of a carbon-carbon bond hydrolase. *Structure* 7, 1023 – 1033.

657 Turner, M., Yang, X., Yin, D., Kuczera, K., Borchardt, R., Howell, P., 2000.
658 Structure and function of S-adenosylhomocysteine hydrolase. *Cell Biochemistry and*
659 *Biophysics* 33. 101 – 125.

660 Viarengo, A., Nott, J. A., 1993. Mechanisms of heavy metal cation homeostasis in
661 marine invertebrates. *Comparative Biochemistry and Physiology, Part C* 104, 355 – 371.

662 Von Damm, K., 1988. Systematics of and postulated controls on submarine
663 hydrothermal solution chemistry. *Journal of Geophysical Research* 93, 4551 – 4561.

Table 1. Identifications of proteins significantly up-regulated in gill of *Bathymodiolus* sp. from Tiamat compared with Knuckers Gaff

Spot #	Identified Protein	Mw (Da)	Fold change	ANOVA <i>p</i>	GI Number	Mascot Score	Matched peptides	Sequence Coverage (%)	Function
479	S-adenosylhomocysteine hydrolase	47498	2.8	0.016	253769244	392	3	22	Cytosolic enzyme involved in cysteine synthesis and consequently glutathione-based redox homeostasis
461	Alpha enolase	40415	2.2	0.007	4416381	122	1	21	Enzyme involved in glycolysis, growth control, hypoxia tolerance, heat shock allergic responses
372	Glutamine synthetase type I	51968	2.0	0.03	345876672	205	2	24	Enzyme specific to prokaryotes, likely from bacterial endosymbionts in mussel gill
773	Actin	28947	1.8	0.01	8895877	566	3	53	Cytoskeleton maintenance; muscle contraction; cell motility; cell signalling; ROS target
478	Fumarylacetoacetate hydrolase	45979	1.6	0.045	157131060	158	2	18	Hydrolase enzyme involved in metabolism of aromatic amino acids

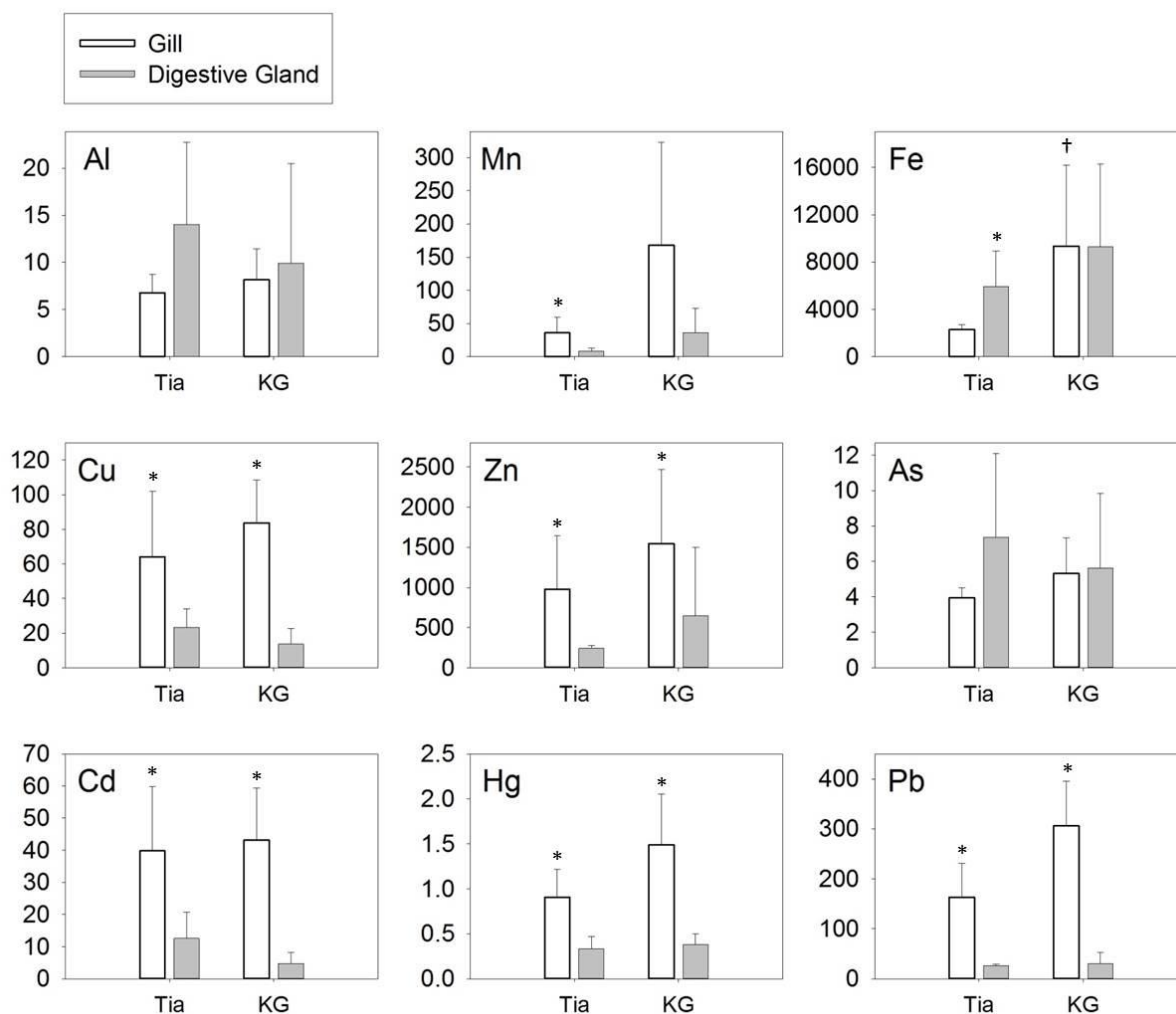


Figure 1. Mean concentration ($\mu\text{g g}^{-1}$ dry weight; $n = 5$) of essential (Mn, Fe, Cu, Zn) and toxic (Al, As, Cd, Hg, Pb) metals in gill (white bars) and digestive gland (grey bars) tissues of *Bathymodiolus* sp. from SW Indian Ridge hydrothermal vent sites; Tiamat (Tia) and Knuckers Gaff (KG). Error bars indicate the standard deviation on the mean. Significant differences between gill and digestive gland are indicated by *, and between sites by †.

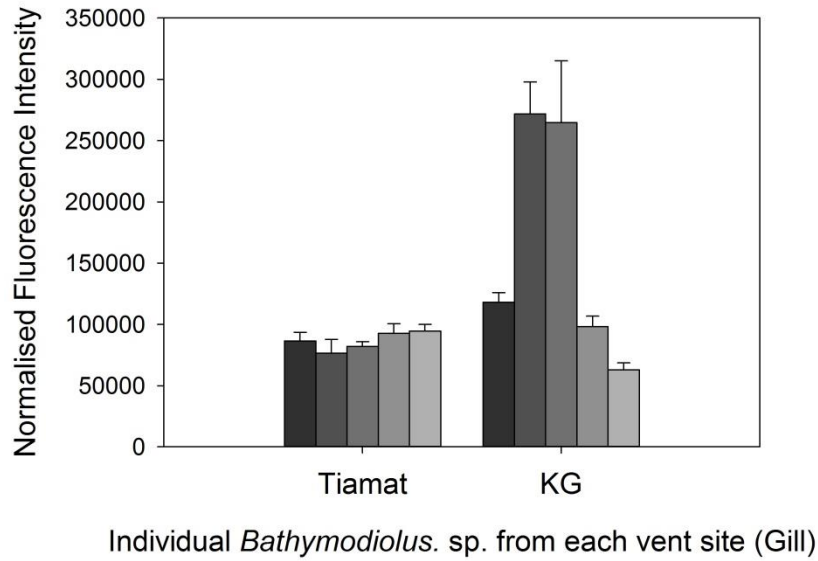


Figure 2. Intensity of fluorescence measured in IAF-labelled gill tissues of *Bathymodiolus* sp. individuals collected from Tiamat (n = 5) and Knuckers Gaff (n = 5) vent sites. Count values are normalised to protein content, as measured by optical density in coomassie-stained gels. Error bars indicate the standard deviation from the mean measured over four technical replicates.

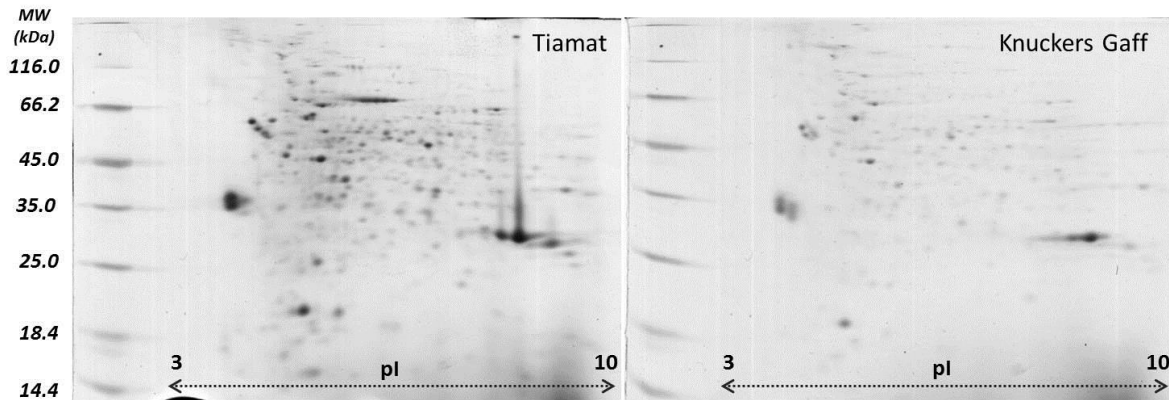


Figure 3. Representative images of electrophoretically separated, coomassie-stained protein spots for *Bathymodiolus* sp. gill tissues sampled from Tiamat and KG vent sites. A protein molecular mass marker ranging from 14.4 kDa (bottom) to > 116.0 kDa (top) is shown for size reference. Isoelectric point (pI) is indicated along the pH range (3-10).

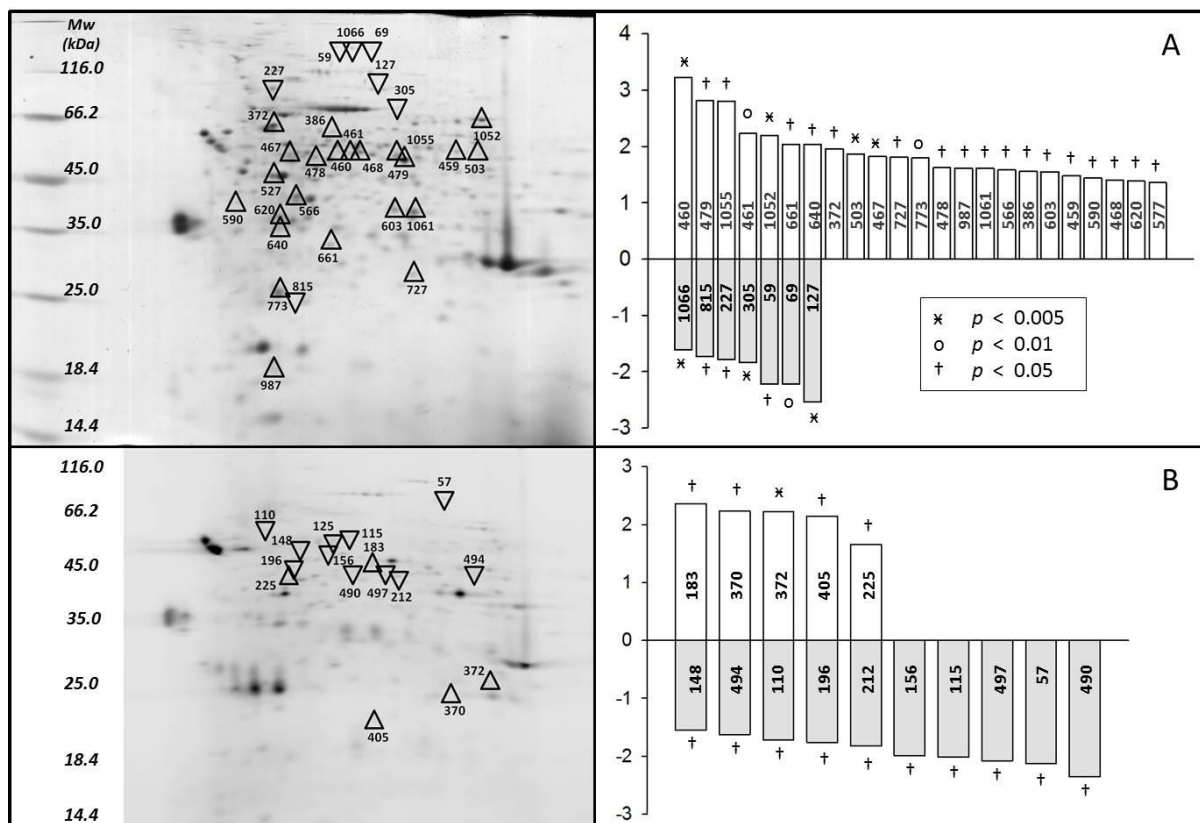


Figure 4. (A: Left) Coomassie-stained and (B: Left) IAF-labelled protein separations of a *Bathymodiolus* sp. gill tissue sample from the Tiamat site. Significant changes in spot intensity, compared with the Knuckers Gaff site, are indicated by upright triangles (greater at Tiamat) and inverted triangles (greater at Knuckers Gaff). A protein molecular mass marker ranging from 14.4 kDa (bottom) to > 116.0 kDa (top) is shown for size reference. (A and B: Right) Fold-differences in spot intensity at Tiamat, in comparison with Knuckers Gaff. Corresponding spot numbers are shown on each vertical bar, and the level of significance (t-test; p value) associated with each fold change is indicated by the symbols *, o, and †.

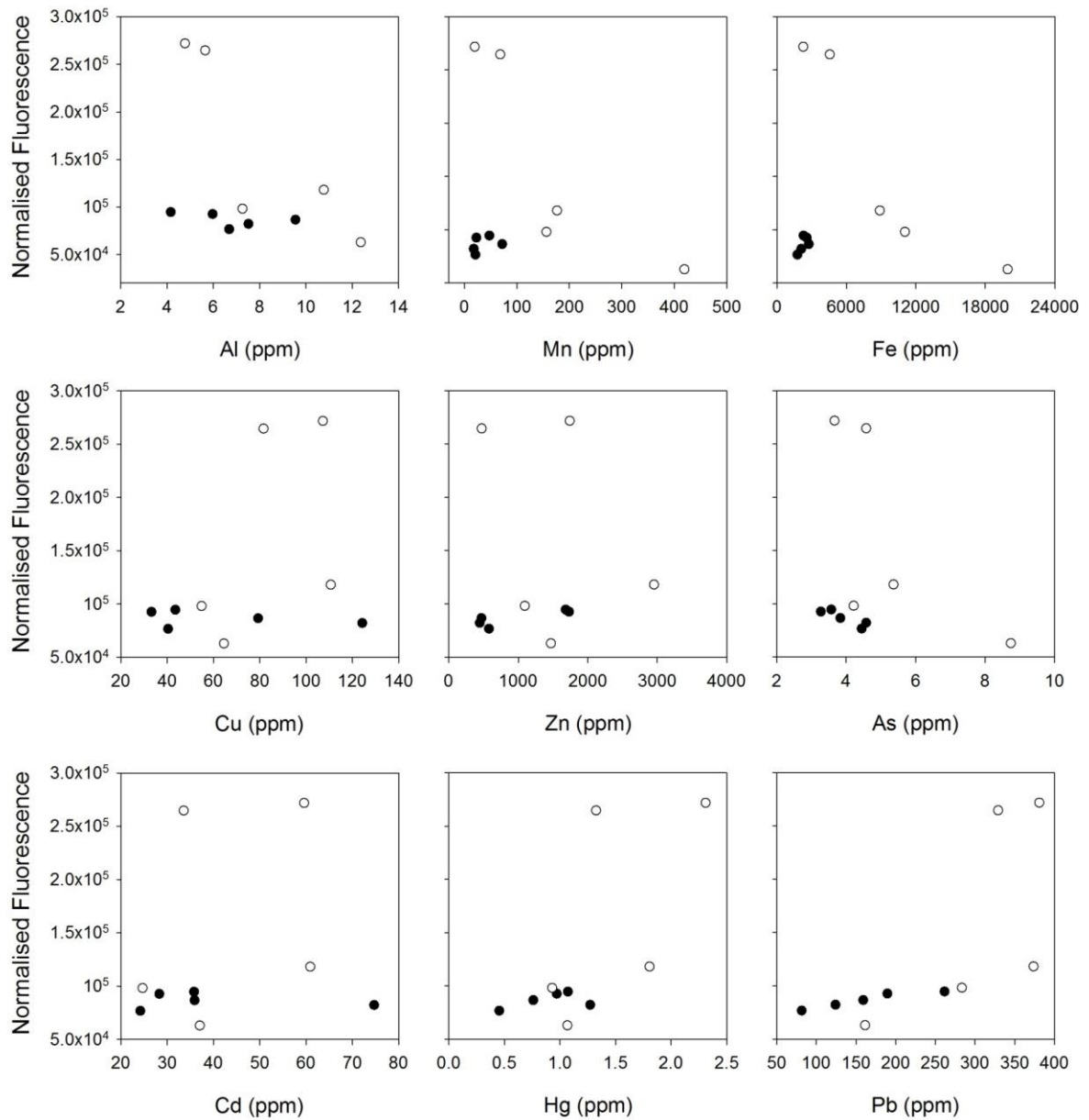


Figure S1. Coomassie-normalised fluorescence intensity for IAF-labelled proteins in relation to metal content in gill tissues of *Bathymodiolus* sp. individuals sampled from Tiamat (black circles) and Knuckers Gaff (white circles) hydrothermal vent sites.